Classical Simulation of Infinite-Size Quantum Lattice Systems in One Spatial Dimension

G. Vidal

School of Physical Sciences, The University of Queensland, QLD 4072, Australia

(Received 19 November 2006; published 12 February 2007)

Invariance under translation is exploited to efficiently simulate one-dimensional quantum lattice systems in the limit of an infinite lattice. Both the computation of the ground state and the simulation of time evolution are considered.

DOI: 10.1103/PhysRevLett.98.070201 PACS numbers: 02.70.−c, 03.67.−a, 71.27.+a

Numerical renormalization group (RG) methods obtained a first remarkable success with Wilson's solution of the Kondo problem [1] and, ever since the irruption of White's density matrix renormalization group (DMRG) algorithm [2], are solidly established as the dominant computational approach to quantum lattice systems in one spatial dimension (1D) [3]. Recently, progress in our understanding of quantum entanglement has prompted a series of new developments [4–9] that extend the domain of RG methods in two main directions. On the one hand, still in the context of 1D lattice systems, the time-evolving block decimation algorithm (TEBD) allows for the simulation of time evolution [4]. On the other, Verstraete and Cirac [5] have introduced projected entangled-pair states (PEPS) to address the simulation of quantum lattice systems in two and higher spatial dimensions.

In this Letter, we propose an algorithm, based on TEBD, to simulate 1D quantum lattice systems in the thermodynamic limit. Bulk properties of matter are best studied in an infinite system, where they are not contaminated by finite-size corrections or boundary effects. However, for most algorithms the cost of a simulation grows with the system size, and the thermodynamic limit can only be reached by extrapolating results for increasingly large systems. Here we exploit two facts, namely, invariance under translations of the system and parallelizability of local updates in TEBD, to obtain a noticeably simple and fast algorithm, referred to as infinite TEBD or iTEBD, to simulate infinite systems directly, without resorting to costly, less accurate extrapolations. We describe the iTEBD algorithm and test its performance by computing the ground state and time evolution for a quantum spin chain in the thermodynamic limit. In addition to offering a very competitive alternative to DMRG for infinite systems, iTEBD plays a key role in entanglement renormalization techniques [10] and in the extension of PEPS [5] to infinite 2D lattices [11].

We consider an infinite array of sites in 1D, where each site r, $r \in \mathbb{Z}$, is described by a complex vector space $V^{[r]} \cong \mathbb{C}^d$ of finite dimension d. Let vector $|\Psi\rangle$ denote a pure state of the lattice and operator $H = \sum_r h^{[r,r+1]}$ a Hamiltonian with nearest-neighbor interactions, where we assume that $|\Psi\rangle$ and H are invariant under shifts by one lattice site [12]. Given an initial state $|\Psi_0\rangle$, our goal is to simulate an evolution according to H, both in real time

$$|\Psi_t\rangle = \exp(-iHt)|\Psi_0\rangle, \tag{1}$$

and in imaginary time [13],

$$|\Psi_\tau\rangle = \frac{\exp(-H\tau)|\Psi_0\rangle}{\| \exp(-H\tau)|\Psi_0\rangle \|}. \tag{2}$$

The TEBD algorithm represents $|\Psi\rangle$ through a matrix product state (MPS) [14]. See [4] for details on this structure, that we briefly review for an infinite 1D lattice. Let $[\lhd r]$ and $[r+1 \rhd]$ denote the semi-infinite sublattices made of sites $\{-\infty, \cdots, r\}$ and $\{r+1, \cdots, \infty\}$. If the Schmidt decomposition of $|\Psi\rangle$ according to this bipartition reads

$$|\Psi\rangle = \sum_{\alpha=1}^{\chi} \lambda_\alpha^{[r]} |\Phi_\alpha^{[\lhd r]}\rangle \otimes |\Phi_\alpha^{[r+1\rhd]}\rangle, \tag{3}$$

where we assume the Schmidt rank χ to be finite, then the spectral decomposition of the reduced density matrices for $[\lhd r]$ and $[r+1\rhd]$ are

$$\rho^{[\lhd r]} = \sum_{\alpha=1}^{\chi} (\lambda_\alpha^{[r]})^2 |\Phi_\alpha^{[\lhd r]}\rangle\langle\Phi_\alpha^{[\lhd r]}|, \tag{4}$$

$$\rho^{[r+1\rhd]} = \sum_{\alpha=1}^{\chi} (\lambda_\alpha^{[r]})^2 |\Phi_\alpha^{[r+1\rhd]}\rangle\langle\Phi_\alpha^{[r+1\rhd]}|. \tag{5}$$

We use a three-index tensor $\Gamma^{[r]}$ to relate the Schmidt bases for two left (right) sublattices:

$$|\Phi_\alpha^{[\lhd r+1]}\rangle = \sum_{\beta=1}^{\chi} \sum_{i=1}^{d} \lambda_\beta^{[r]} \Gamma_{i\beta\alpha}^{[r+1]} |\Phi_\beta^{[\lhd r]}\rangle |i^{[r+1]}\rangle, \tag{6}$$

$$|\Phi_\alpha^{[r\rhd]}\rangle = \sum_{\beta=1}^{\chi} \sum_{i=1}^{d} \Gamma_{i\alpha\beta}^{[r+1]} \lambda_\beta^{[r+1]} |i^{[r]}\rangle |\Phi_\beta^{[r+1\rhd]}\rangle. \tag{7}$$

In particular, $|\Psi\rangle$ can be expanded in the local basis $|i^{[r]}\rangle$ for site r and in terms of $\lambda^{[r]}\Gamma^{[r+1]}\lambda^{[r+1]}$ as

$$|\Psi\rangle = \sum_{\alpha,\beta=1}^{\chi} \sum_{i=1}^{d} \lambda_\alpha^{[r]} \Gamma_{i\alpha\beta}^{[r+1]} \lambda_\beta^{[r+1]} |\Phi_\alpha^{[\lhd r]}\rangle |i^{[r]}\rangle |\Phi_\alpha^{[r+1\rhd]}\rangle, \tag{8}$$

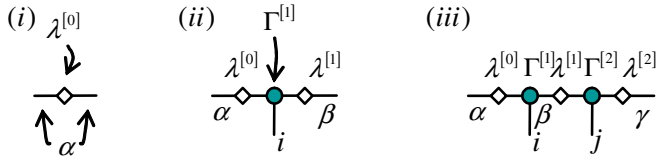

FIG. 1 (color online). Diagrammatic representation of several decompositions of $|\Psi\rangle$ in terms of a network of tensors, see [8] for more details. Each filled circle represents a tensor Γ and each edge represents an index, such as α or i. Hanging from an open side of an edge there is an (omitted) orthonormal basis, such as $|\Phi_\alpha^{[\lhd 0]}\rangle$ or $|i^{[1]}\rangle$. An open diamond on top of an edge represents a set of weights λ (Schmidt coefficients) for the corresponding index. (i) Schmidt decomposition, Eq. (3), according to semi-infinite sublattices $[\lhd 0]$ and $[1\rhd]$. The bases $|\Phi_\alpha^{[\lhd 0]}\rangle$ and $|\Phi_\alpha^{[1\rhd]}\rangle$ are linked through index α with weights $\lambda_\alpha^{[0]}$. (ii) Expansion of $|\Psi\rangle$ in terms of the Schmidt bases for the semi-infinite sublattices $[\lhd 0]$ and $[2\rhd]$ and an orthonormal basis for site 1; see Eq. (8). (iii) Expansion of $|\Psi\rangle$ in terms of orthonormal sets of vectors for sublattices $[\lhd 0]$ and $[3\rhd]$ and sites 1 and 2.

or for sites $\{r, r+1\}$ in terms of $\lambda^{[r]}\Gamma^{[r+1]}\lambda^{[r+1]}\Gamma^{[r+2]}\lambda^{[r+2]}$, and so on; see Fig. 1. We also recall that in the TEBD algorithm the evolution operator $\exp(-iHt)$ in Eq. (1) is expanded through a Suzuki-Trotter decomposition [15] as a sequence of small two-site gates

$$U^{[r,r+1]} \equiv \exp(-ih^{[r,r+1]}\delta t), \qquad \delta t \ll 1, \tag{9}$$

which we arrange into gates U^{AB} and U^{BA},

$$U^{AB} \equiv \bigotimes_{r\in\mathbb{Z}} U^{[2r,2r+1]}, \qquad U^{BA} \equiv \bigotimes_{r\in\mathbb{Z}} U^{[2r-1,2r]}. \tag{10}$$

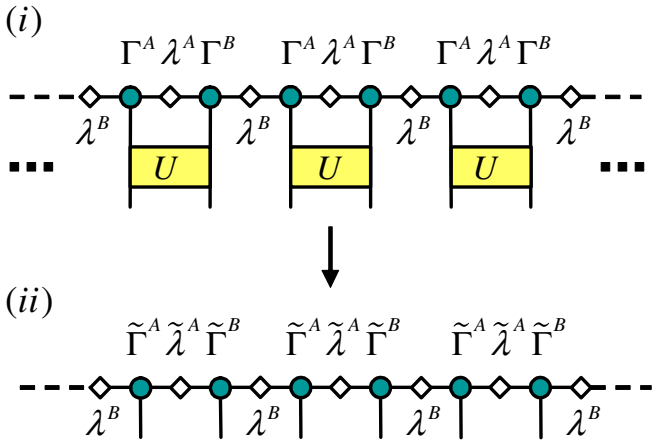

FIG. 2 (color online). Two diagrammatical representations (see also Fig. 1 and Ref. [8]) for state $U^{AB}|\Psi\rangle$: (i) tensor network representation containing both an MPS for $|\Psi\rangle$ and two-site gates U acting on each pair of sites $\{2r, 2r+1\}$, $\forall\ r \in \mathbb{Z}$; (ii) new MPS for $U^{AB}|\Psi\rangle$. Notice that both structures are invariant under shifts by two lattice sites and are completely specified by a small number of tensors, in spite of the fact that they represent a state of an infinite 1D lattice.

Because state $|\Psi\rangle$ is shift invariant, it could be represented with a MPS where $\Gamma^{[r]}$ and $\lambda^{[r]}$ are independent of r. However, we will partially break translational symmetry to simulate the action of gates (10) on $|\Psi\rangle$. Accordingly, we choose a MPS of the form

$$\begin{aligned} \Gamma^{[2r]} &= \Gamma^A, \qquad \lambda^{[2r]} = \lambda^A, \\ \Gamma^{[2r+1]} &= \Gamma^B, \qquad \lambda^{[2r+1]} = \lambda^B, \qquad r \in \mathbb{Z}. \end{aligned} \tag{11}$$

As in the finite n case [4], the simulation of the time evolution, see Eq. (1), is achieved by updating the MPS so as to account for the repeated application of gates U^{AB} and U^{BA} on $|\Psi\rangle$. But for $n = \infty$, the action of the gates preserves the invariance of the evolved state under shifts by two sites (see Fig. 2), and only tensors Γ^A, Γ^B, λ^A, and λ^B need to be updated—a task that is achieved through simple matrix manipulations; see Fig. 3. In other words, whereas for n sites the TEBD algorithm requires $O(nd\chi^2)$ space to store an MPS and $O(nd^3\chi^3)$ time to simulate a small evolution $\exp(-iH\delta t)$ [4], for $n = \infty$ sites the iTEBD requires computational space and time that scale just as $O(d^2\chi^2)$ and $O(d^3\chi^3)$. The key to such dramatic cost reduction by a factor n is the fact that, in contrast to other approaches [6], we use a MPS based on the Schmidt decomposition, allowing for a parallelized, local update of tensors Γ and λ.

Finally, evolution in imaginary time, Eq. (2), is also simulated with iTEBD by simply replacing the two-site unitary gates $\exp(-ih\delta t)$ in Eq. (9) with nonunitary gates $\exp(-h\delta\tau)$, $\delta\tau \ll 1$ [16].

We have tested the performance of iTEBD by computing the ground state and by simulating time evolution for the 1D quantum Ising chain with transverse magnetic field, as

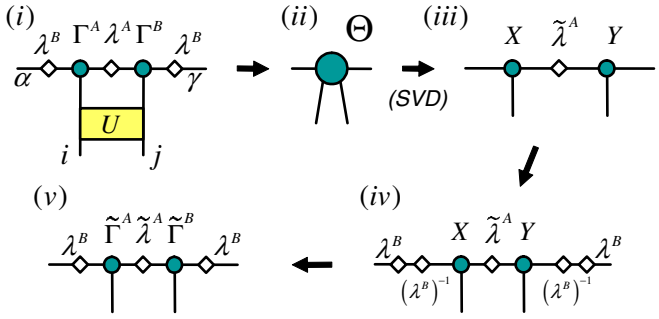

FIG. 3 (color online). In order to update the MPS after gate U has been applied, see Fig. 2, we first contract the tensor network (i) into a single tensor $\Theta_{\alpha ij\gamma}$ (ii). We then compute the singular value decomposition of Θ according to the index bipartition $[\alpha i]$:$[j\gamma]$, namely, $\Theta = \sum_\beta X_{[\alpha i]\beta}\tilde{\lambda}^A_\beta Y_{\beta[j\gamma]}$ as in (iii). We introduce λ^B back into the network (iv) and form tensors $\tilde{\Gamma}^A$ and $\tilde{\Gamma}^{[B]}$ in (iv) by attaching to X and Y the inverse of the Schmidt coefficients λ^B. All such matrix manipulations are achieved with $O(d^2\chi^2)$ space and $O(d^3\chi^3)$ and need to be performed only once in order to update the MPS for the whole infinite chain.

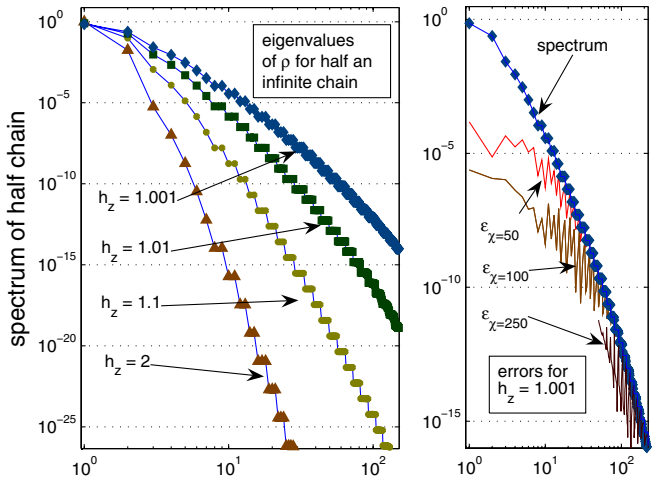

FIG. 4 (color online). Left: spectrum $p_\alpha = (\lambda_\alpha)^2$ of the density matrix for half of the infinite chain, see Eq. (4), for different values of the magnetic field h_z. For $h_z \gg 1$ the eigenvalues p_α decay very fast with α. As h_z approaches the critical value $h_z^* = 1$, the decay is less pronounced and the computation of the spectrum becomes more demanding. Right: however, for $h_z = 1.001$ we still obtain the 50, 100, and 250 first eigenvalues with remarkable accuracy, the error on p_α being typically several orders of magnitude smaller than its value.

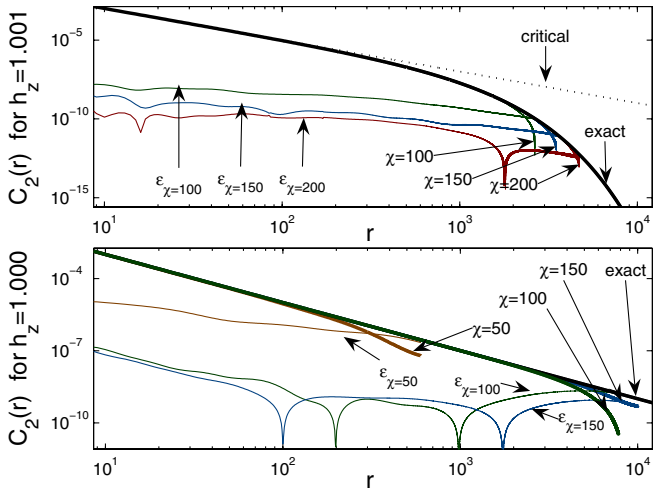

FIG. 5 (color online). Two-point correlator $C_2(r)$ of Eq. (13). Upper part: for $h_z = 1.001$, when the distance r between spins is up to several hundred sites, $C_2(r)$ seems to decay as a power law (as in the critical case), but for r of the order of 1000, the exponential character of the decay becomes manifest. Lower part: even though iTEBD is unable to properly reproduce the spectrum p_α of half an infinite chain at criticality, $h_z = 1$, (see Fig. 4), we still obtain a very accurate approximation to the correlator $C_2(r)$ when r is of the order of several thousands of spins.

defined by the Hamiltonian

$$H = \sum_{r\in\mathbb{Z}} (\sigma_x^{[r]}\sigma_x^{[r+1]} + h_z\sigma_z^{[r]}). \tag{12}$$

This model is exactly solvable [17], allowing for a direct comparison of numerical results with the exact solution.

First, by simulating an evolution in imaginary time, Eq. (2), we have obtained an approximate MPS representation of the ground state $|\Psi_g\rangle$ for several values of $h_z \geq 1$. We assess the accuracy of the result by focusing on the following: (i) the spectrum $p_\alpha = (\lambda_\alpha^{[r]})^2$ of the reduced density matrix for half the infinite lattice, Eq. (4), which characterizes entanglement across the boundary of two halves of the chain; and (ii) the two-point correlator

$$C_2(r) \equiv \langle\Psi_g|\sigma_z^{[0]}\sigma_z^{[r]}|\Psi_g\rangle - (\langle\Psi_g|\sigma_z^{[0]}|\Psi_g\rangle)^2, \tag{13}$$

which quantifies the strength of correlations between two spins that are r lattice sites apart.

In both cases, we obtain quantitative agreement with the exact solution up to several significant digits, see Figs. 4 and 5. Computing the ground state $|\Psi_g\rangle$ is particularly fast and accurate for large values of h_z (say $h_z \geq 1.1$) and, as expected, becomes more resource intensive as h_z approaches the critical value $h_z^* = 1$ [18]. We find, however, that for values very close to the critical point, such as $h_z = 1.001$, we still obtain accurate approximations to the half-chain spectrum $\{p_\alpha\}$ and the correlator $C_2(r)$ through affordable simulations, see Fig. 5. And, most remarkably, reliable results for $C_2(r)$ are obtained even at the critical point $h_z = 1$ by using a MPS with a reasonably small χ, in spite of the fact that such a MPS is no longer able to reproduce $\{p_\alpha\}$.

Second, by switching to real time, we have simulated the evolution of the infinite system, prepared in the ground state of H in Eq. (12) for $h_z = 10$, when the magnetic field is abruptly modified from its initial value to $h_z' = 3$. Figure 6 shows the evolution in time of the magnetization

$$m_z(t) \equiv \langle\Psi_g|\sigma_z^{[1]}|\Psi_g\rangle, \tag{14}$$

which after several oscillations becomes stable at some value different from the initial one.

Summarizing, with modest computational resources, the iTEBD is able to analyze an infinite 1D system, near to and at a quantum critical point, for which it obtains accurate results for quantities involving up to several thousands of sites. A fair comparison with previous algorithms [2,4,6] involves many considerations and will be addressed elsewhere. We notice, however, that reproducing the above results with, say, the infinite-size DMRG algorithm [2], would require analysing a system with several thousands of sites, with computational cost that scales at least linearly in the number of sites. Work in progress considers a range of applications of the iTEBD, including the characterization of quantum critical points and crossover between quantum phases, and the study of the response of 1D systems to external probes. Originally developed to help in the context

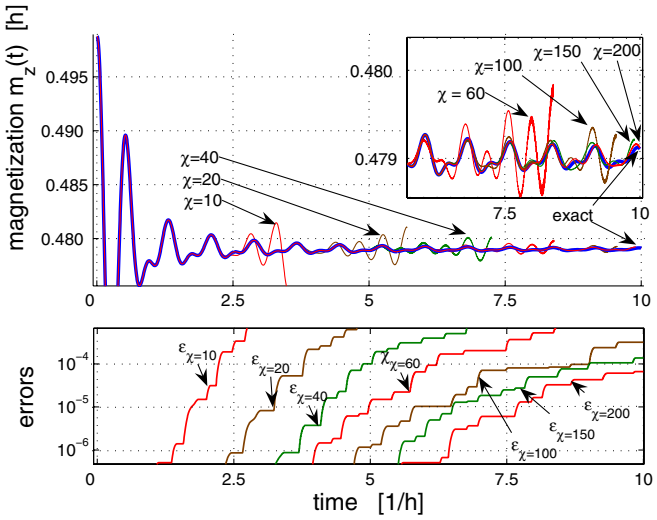

FIG. 6 (color online). Simulation of the evolution in time of $m_z(t)$ in Eq. (14). The infinite chain is initially in the ground state of H with $h_z = 10$. At $t = 0$ the magnetic field is changed to $h_z = 3$. Upper part: the magnetization, originally at a value $m_z(0) \approx 0.5$, oscillates in time until it stabilizes around a lower value $m_z(\infty) \approx 0.48$. By considering increasingly large values of χ we are able to simulate the evolution of $m_z(t)$ for long times with remarkable accuracy. Lower part: scaling of errors with time for different values of χ.

of entanglement renormalization [10], the method is also the key to extend 2D PEPS [5] to infinite systems [11].

The author acknowledges support from the Australian Research Council (Project FF0668731).

[1] K. Wilson, Phys. Rev. B **4**, 3184 (1971).
[2] S. R. White, Phys. Rev. Lett. **69**, 2863 (1992); Phys. Rev. B **48**, 10 345 (1993).
[3] U. Schollwoeck, Rev. Mod. Phys. **77**, 259 (2005).
[4] G. Vidal, Phys. Rev. Lett. **91**, 147902 (2003); **93**, 040502 (2004); S. R. White and A. E. Feiguin, Phys. Rev. Lett. **93**, 076401 (2004); A. J. Daley *et al.*, J. Stat. Mech. (2004) P04005.
[5] F. Verstraete and J. I. Cirac, cond-mat/0407066.
[6] F. Verstraete, J. J. Garcia-Ripoll, and J. I. Cirac, Phys. Rev. Lett. **93**, 207204 (2004); B. Paredes, F. Verstraete, and J. I. Cirac, cond-mat/0505288; F. Verstraete, D. Porras, and J. I. Cirac, Phys. Rev. Lett. **93**, 227205 (2004); D. Porras, F. Verstraete, and J. I. Cirac, cond-mat/0504717.
[7] M. Zwolak, and G. Vidal, Phys. Rev. Lett. **93**, 207205 (2004).
[8] Y. Y. Shi, L. M. Duan, and G. Vidal, quant-ph/0511070.
[9] T. Osborne, quant-ph/0601019; quant-ph/0603137; cond-mat/0605194.
[10] G. Vidal, cond-mat/0512165; quant-ph/0610099.
[11] J. Jordan *et al.*, (in preparation).
[12] Simple extensions of the algorithm include: (i) interactions $h^{[r,s]}$ with longer range, $|r - s| > 1$, (ii) interactions involving more than just two sites (e.g., $h^{[r,s,t,\ldots]}$), (iii) time-dependent Hamiltonians, and (iv) systems invariant under shifts by m sites, with $m > 1$.
[13] For a finite lattice with n sites and a Hamiltonian H with gap $\Delta > 0$, simulating imaginary time evolution as in Eq. (2) for large τ yields a good approximation $|\Psi_\tau\rangle$ to the ground state $|\Psi_g\rangle$ of H, since one can show that

$$|\langle\Psi_\tau|\Psi_g\rangle| > 1 - O\left(\frac{e^{-2\Delta\tau}}{\delta^2}\right), \qquad \delta \equiv |\langle\Psi_0|\Psi_g\rangle|. \quad (15)$$

Notice that Eq. (15) may becomes meaningless in the limit $n \to \infty$, where typically $\delta \to 0$, or for a gapless Hamiltonian, $\Delta = 0$. Here we will not provide a justification for the validity of TEBD as a method to approximate $|\Psi_g\rangle$ in the $n \to \infty$ and/or $\Delta = 0$ regimes, but refer instead to successful benchmark calculations.
[14] M. Fannes, B. Nachtergaele, and R. F. Werner, Commun. Math. Phys. **144**, 443 (1992); S. Östlund and S. Rommer, Phys. Rev. Lett. **75**, 3537 (1995).
[15] M. Suzuki, Phys. Lett. A **146**, 319 (1990); J. Math. Phys. (N.Y.) **32**, 400 (1991); For third and forth order expansions, see also A. T. Sornborger and E. D. Stewart, quant-ph/9809009.
[16] Nonunitary gates destroy the Schmidt decomposition and a parallelized, local update of tensors (11) should no longer be possible. For small $\delta\tau$, however, gate $\exp(-h\delta\tau)$ is close to the identity, and proceeding with a local update introduces only small errors that vanish as $\delta\tau \to 0$. An accurate MPS for the ground state $|\Psi_g\rangle$ is then achieved by simulating imaginary time evolution with decreasingly small values of $\delta\tau$.
[17] P. Pfeuty, Ann. Phys. (N.Y.) **57**, 79 (1970); E. Barouch and B. M. McCoy, Phys. Rev. A **3**, 786 (1971).
[18] The simulations were performed using the MATLAB code in a laptop with a 2 GHz processor and 1 GB of RAM. An approximation to the ground state of H in Eq. (12) was computed through an evolution in imaginary time until convergence of the spectrum $\{p_\alpha\}$. We used a fourth order Suzuki-Trotter expansion [15], with decreasing values of $\delta\tau \in \{0.1, 0.01, 0.001, \cdots\}$. For $h_z = 1.1$ with $\chi = 50$, convergence of the spectrum was achieved after just a few seconds, whereas the case $h_z = 1.01$ with $\chi = 100$ required a few minutes and the case $h_z = 1.001$ with $\chi = 200$ required a few hours. At criticality, $h_z = 1$ and $\chi = 150$, no convergence of the spectrum was achieved after a few days. However, just after a few hours, the resulting MPS was able to accurately reproduce the correlator $C_2(r)$ for $r \leq 5000$ sites.